c[D-pro-Pro-D-pro-*N*-Methyl-Ala] Adopts a Rigid Conformation That Serves As a Scaffold to Mimic Reverse-Turns

Sage Arbor,[1] Jeff Kao,[2] Yun Wu,[1] Garland R. Marshall[1]
[1]*Department of Biochemistry and Molecular Biophysics, Washington University, St. Louis, MO 63110*
[2]*Department of Chemistry, Washington University, St. Louis, MO 63110*

Received 14 July 2007; revised 20 September 2007; accepted 5 October 2007
Published online 16 October 2007 in Wiley InterScience (www.interscience.wiley.com). DOI 10.1002/bip.20869

ABSTRACT:

Naturally occurring cyclic tetrapeptides (CTPs) such as tentoxin (Halloin et al., Plant Physiol 1970, 45, 310–314; Saad, Phytopathology 1970, 60, 415–418), ampicidin (Darkin-Rattray, Proc Natl Acad Sci USA 1996, 93, 13143–13147), HC-toxin (Walton, Proc Natl Acad Sci USA 1987, 84, 8444–8447), and trapoxin (Yoshida and Sugita, Jpn J Cancer Res 1992, 83, 324–328; Itazaki et al., J Antibiot (Tokyo) 1990, 43, 1524–1532) have a wide range of biological activity and potential use ranging from herbicides (Walton, Proc Natl Acad Sci USA 1987, 84, 8444–8447; Judson, J Agric Food Chem 1987, 35, 451–456) to therapeutics (Loiseau, Biopolymers 2003, 69, 363–385) for malaria (Darkin-Rattray, Proc Natl Acad Sci USA 1996, 93, 13143–13147) and cancer (Yoshida and Sugita, Jpn J Cancer Res 1992, 83, 324–328). To elucidate scaffolds that have few low-energy conformations and could serve as semirigid reverse-turn mimetics, the flexibility of CTPs was determined computationally. Four analogs of cyclic tetraproline c[Pro-pro-Pro-pro] with alternating L- and D-prolines, namely c[pro-Pro-pro-NMe-Ala], c[pip-Pro-pip-Pro], c[pro-Pip-pro-Pro], and c[Ala-Pro-pip-Pro] were synthesized and characterized by NOESY NMR. Both molecular mechanics and Density Functional Theory quantum calculations found these head-to-tail CTPs to be constrained to one or two relatively stable conformations. NMR structures, while not always yielding the same lowest energy conformation as expected by in silico predictions, confirmed only one or two highly populated solution conformations for all four peptides examined. c[pro-Pro-pro-NMe-Ala] was shown to have a single all trans*-amide bond conformation from both in silico predictions and NMR characterization, and to be a reverse-turn mimetic by overlapping four Cα-Cβ bonds with those for ~6.5% (Tran, J Comput Aided Mol Des 2005, 19, 551–566) of reverse-turns in the Protein Data Bank PDB with a RMSD of 0.57 Å.* © *2007 Wiley Periodicals, Inc. Biopolymers (Pept Sci) 90: 384–393, 2008.*

Keywords: cyclic tetrapeptide; privileged scaffold; conformation; proline; pipecolic acid

This article was originally published online as an accepted preprint. The "Published Online" date corresponds to the preprint version. You can request a copy of the preprint by emailing the Biopolymers editorial office at biopolymers@wiley.com

Correspondence to: Garland R. Marshall, Washington University – Biochemistry and Molecular Biophysics, Center for Computational Biology, 700 S. Euclid Ave., St. Louis, Missouri 63110; USA; e-mail: garland@pcg.wustl.edu or garlandm@gmail.com
Contract grant sponsor: NIH
Contract grant number: GM 68460
This article contains supplementary material available via the Internet at http://www.interscience.wiley.com/jpages/0006-3525/suppmat.

INTRODUCTION

Two common problems in developing therapeutics are determining an accurate binding mode of ligands being mimicked and finding rigid structures that accurately mimic the geometry of molecular recognition. Both of these problems can be addressed by developing libraries of privileged scaffolds that mimic the

well defined tertiary structure in macromolecules. Screening of these privileged scaffolds libraries would help determine how ligand side chains are stabilized upon binding as well as establish lead compounds for therapeutic optimization. Reverse turns, which have been found to make up one-fourth of the residues in high-resolution protein structures in the Protein Data Bank (PDB)[1] are often viewed as targets for therapeutic design[2,3] because they are generally found on the exterior of proteins and often involved in macromolecule interactions.[4,5] Reverse turns are characterized by a four-residue sequence that creates a $\sim 180^\circ$ turn in the polypeptide chain, with the first and fourth Cα atoms within 7 Å. As a subclass of reverse turns, classical β-turns,[5] contain a hydrogen bond between the first residue's carbonyl oxygen and the fourth residue's amide hydrogen. Rigid compounds that have modifiable bonds overlapping Cα-Cβ bonds in reverse turns, such as benzodiazapenes,[6–11] can be considered privileged mimetic scaffolds; they can bind to molecular recognition sites for reverse turns with the potential for high affinity due to their preorganization.[6–8,11]

Two methods used to nucleate reverse-turn structures incorporate a sequence of either pro-Pro or Pro-pro at the i+1 and i+2 positions[12–14] of the turn, or use small cyclic peptides either cyclized through side chains or head-to-tail.[5,7,15,16] Cyclic peptides are widely investigated for therapeutic use due to their rigid scaffold and bioavailability.[17] Cyclic peptides, such as θ-Defensins, naturally occur in many organisms and have a broad range of activity, acting as antibiotics or antivirals for HIV-1, herpes simplex, or influenza A viruses.[18] Cyclic tetrapeptides (CTPs), ampicidin,[19] HC-toxin,[20] and trapoxin[21,22] all have been found to be inhibitors of histone deacetylase which control the expression of genes. These CTPs are therefore thought to be possibly useful as cancer therapeutics. CTPs seem particularly apt at mimicking reverse turns in that they inherently have a main chain that turns $\sim 180^\circ$ four consecutive times in four residues.

Combining two approaches by incorporating pro-Pro or Pro-pro sequences into a CTP should yield conformationally constrained reverse-turn mimetics.[23] Because of their macrocyclic ring constraint, the conformation of head-to-tail CTPs can largely be described by the *cis/trans*-conformation of their backbone amide bonds. Unlike cyclic tripeptides and pentapeptides which contain either only *cis*-, or largely *trans*-amide bonds, respectively, CTPs contain a mixture of both *cis*- and *trans*-peptide bonds.[24] This "sweet spot" of CTPs seems ideal for fine tuning of various rigid structures since the positions of *cis/trans*-amide bonds largely determines the conformation of the mimetic scaffold. The CTP c[Pro-pro-Pro-pro] is a combination of these two reverse-turn mimetic approaches shown to exist with stable *cis-trans-cis-trans* and *trans-cis-trans-cis* amide bond conformers at room temperature in water.[25,26] In this study, we modified the CTP c[Pro-pro-Pro-pro] by substituting L- or D-proline with alanine, *N*-methyl-alanine (NMe-Ala), or L- or D-pipecolic acid (Pip) to stabilize other sets of amide conformations such as *trans-trans-trans-trans* and *trans-trans-cis-trans*. Different sequences of amide-bond torsions, which dictates the backbone-ring conformations, changes the relative orientation of the proline and Pip rings enabling them to act as mimics for multiple turn types. CTPs macrocycles tend to either a boat or chair conformation, in a similar fashion to cyclohexane.[26,27] To use CTPs as effective turn mimics, this boat or chair conformation must be known. In addition the various macrocycles have different dipoles that might impact binding to different receptors. Cylic peptide reverse-turn mimics which have a proline or pipecolic residue have the added benefit that the side-chain exocyclic ring can be used to rigidify bonds (χ_1, χ_2, etc.) distal to the Cα-Cβ of the synthetic side chain. For these reasons, it would be useful to have multiple CTPs representing each turn type. Screening a large library of such geometrically constrained molecular probes should assist in identification of the relative orientation of the side chains of the bioactive peptides involved in molecular recognition of a reverse turn at a given receptor.

METHODS

Computational Conformational Searches

The conformational effects of three noncoded D-and L-amino acids (*N*-methyl-alanine (NMe-Ala), pipecolic acid (Pip), and aminoisobutyric acid (Aib)) have on CTPs (Table I) were examined through a Monte-Carlo Multiple Minimum (MCMM) conformational search.[28,29] Searches were done in both vacuum and water using the GB/SA implicit solvation model.[30] 10,000 conformational steps were taken and all structures within 200 kJ were retained in order to validate sampling and the extent of coverage of conformational hyperspace. All 12 bonds in the CTP macrocycle were allowed to rotate, including the four amide bonds. In addition, proline and Pip residues used one and two rotatable bonds to accomodate puckering and chair/boat sampling of side-chain rings, respectively. All calculations were done with Macromodel 7.2[31] with the OPLS2001 Force Field and charges.[32,33] Results are shown in Table I.

Quantum Minimizations

Because the 12-membered macrocycle of CTPs are highly constrained, their amide bonds can be distorted significantly from the ideal 180° (*trans*) or 0° (*cis*) torsions. Density Functional Theory (DFT) minimizations were performed both in vacuo and water on the lowest energy and second-lowest energy conformers found from the MCMM search (Table I). DFT calculations were done using Gaussian98 at the B3LYP/6-31G* level and all aqueous estimations were done using the Onsanger model.[34,35]

Table I Cyclic Tetrapeptide Conformational Searches and NMR Conformations

	ΔΔ*G* Low Energy – 2nd Lowest Energy Conformation (kcal)						
Cyclic Peptide	MCMM Vacuum	MCMM Water	DFT Vacuum	DFT Water	Conf Vac	Conf H_2O	NOESY NMR
c[Pro-Aib-Pro-pro]	5.89	1.88	2.13	1.08	cttt	ctct	—
c[Pro-Aib-Pro-Aib]	5.83	11.71	0.4	4.83	ctct	ctct	—
c[Pro-Aib-Aib-pro]	6.82	20.77	0.84	9.26	tctt	tctt	—
c[Pro-nma-Pro-nma]	1.37	4.29	−6.53	−0.74	tccc	tccc	—
c[Pro-pro-Pip-pip]	9.73	2.73	15.19	9.93	tttt	tttt	—
c[pro-Pro-nma-Nma]	1.23	0.9	—	—	tctt	ctcc	—
c[pro-Pro-pro-Nma]	6.8	0.34	7.52	5.33	tttt	tttt	tttt
c[pro-Pip-pro-Pro]	8.27	0.93	12.24	5.31	tttt	tttt	t-t-
c[pip-Pro-pip-Pro]	9.43	1.63	16.96	7.98	tttt	tttt	ttct
c[Ala-Pro-pip-Pro]	2.32	1.66	—	—	tttc	tttc	ttct

Cyclic peptides were conformationally searched both in vacuum and water by the Monte Carlo Multiple Minimum (MCMM) algorithm. The ΔΔ*G* (kcal) between the lowest-energy and second-lowest energy conformer was calculated and the lowest-energy amide bond conformation found is listed. These two conformers were minimized using Density Functional Theory (DFT) in vacuum and water, the ΔΔ*G* between the conformations is listed (kJ), (t, *trans*; c, *cis*, first letter refers to amide bond between first and second amino acid in first column). The four peptides that were synthesized and characterized by NOESY NMR have their experimentally determined amide-bond conformations listed. (Ala, L-Alanine, Pro, L-Proline; pro, D-proline; Aib, aminoisobutyric acid; NmA, *N*-methyl-L-Alanine; nma, *N*-methyl-D-alanine; Pip, L-pipecolic acid; pip, D-pipecolic acid).

Peptide Synthesis, Purification, and Characterization

All peptides were synthesized by solid phase peptide synthesis. 2-Cl-Trityl resin (GL Biochem, Shanghai) was used and substituted with 2*M* equivalents Fmoc-Pro and 5*M* equivalents DIEA in 8 mL *N*,*N*-dimethylformamide (DMF)/g resin and shaken for 30 min, followed by a DCM/DIEA/MeOH 16:3:1 wash to cap the unreacted trityl groups. This yielded a 0.5 m*M* loaded Fmoc-Pro-trityl-resin. Coupling of amino acid residues was done in the presence of 3*M* equivalents. Fmoc-protected amino acids, benzotriazol-1-yloxytris(dimethylamino) phosphonium hexafluorophosphate (BOP), 1-hydroxybenzotriazole (HOBt), and 6*M* equivalents of DIEA were premixed in a minimum of DMF on ice for 5 min and then added to resin bound peptide. After 2–3 h on a shaker for each coupling, removal of the Fmoc protecting group was done with 22% piperidine in DMF for 2 × 10 min. Coupling was monitored by the chloranil test[36] for secondary amines (Pro, Pip, NMe-Ala) and the ninhydrin[36] test for primary amines and a second recoupling performed if required. Peptides were cleaved form the trityl resin with 2% trifluoroacetic acid (TFA) in DCM for 5 min.

Purification of all peptides was done on a Rainin XPHL HPLC system with a Dynamax UV lamp, using a Vydac 218TP1022 (C18, 10 μm, 2.2 cm ID × 25 cm L) RP-HPLC column. All peptides were purified in a A = 100% H_2O and B = 90% ACN/10% H_2O solvent system at a speed of at 10 mL/min. Linear and cyclic peptides were purified in 0.025% HCl and 0.025% TFA solvents, respectively. Cyclizations were carried out in presence of 3*M* equivalents of BOP, HOBt, and 6*M* equivalent DIEA at a 0.5 mg/mL (∼0.1 m*M*) dilution in DMF and shaken for 3 days. Cyclization was followed by TLC, and if incomplete, PyBOP was added for one additional day which greatly facilitated some cyclizations. The solution was then dried by rotary evaporation and dissolved in 1:1 H_2O/ACN for RP-HPLC purification. MS was done on a Finnigan LCQ Classic LC/MS with ion trap and liquid infusion. Because of the lack of ionizable atoms, the cyclic peptides mass spectra mainly appeared as a mixture of cyclic monomers with Na and ionic dimers with Na. The monomer became more apparent, and the ionic dimer vanished in the mass spectra when the CTP solution was greatly diluted (Supplementary Material).

c[pro-Pro-pro-NMe-Ala]. The linear peptide NH_2-pro-NMe-Ala-pro-Pro-COOH was synthesized by standard SPPS as described above by coupling Fmoc-D-pro, Fmoc-N-Me-L-Ala, and Fmoc-D-pro consecutively to L-Pro-trityl-resin. After removal of the N-terminal Fmoc group, the linear tetrapeptide was released from the resin support by treatment with 2% TFA in DCM followed by purification on RP-HPLC. After a 3-day cyclization with HOBt, 3*M* equivalents of PyBOP and DIEA were added for one additional day. The linear and cyclic peptide were purified in a 10–90% B gradient over 15 min and eluted at 9.0 and 15.2 min, respectively, with a 11% overall yield for the pure CTP. Linear NH_2-pro-NMe-Ala-pro-Pro-COOH: ESI-TOF/MS: (*m/z*) Calcd for $C_{19}H_{30}N_4O_5H$ [M + H+], $C_{19}H_{30}N_4O_5Na$ [M + Na+]: 395.48 and 417.47, respectively. Obsd 395.3, 417.4, respectively. c[pro-Pro-pro-NMe-Ala] was analyzed by ^{1}H, COSY, TOCSY, NOESY NMR (500 MHz, CDCL3, −20C) Table II; ESI-TOF/MS: (*m/z*) Calcd for $2(C_{19}H_{28}N_4O_4)H$ [(D + H)+], $2(C_{19}H_{28}N_4O_4)Na$ [(D + Na)+]: 753.91, 775.90, respectively. Obsd 753.6, 775.7, respectively.

c[pro-Pip-pro-Pro]. The linear peptide NH_2-pro-Pip-pro-Pro-COOH was synthesized by standard SPPS as described above by coupling Fmoc-D-pro, Fmoc-L-Pip, and Fmoc-D-pro consecutively to L-Pro-trityl-resin. After removal of the *N*-terminal Fmoc group, the linear tetrapeptide was released by treatment with 2% TFA in DCM from the resin support followed by purification on RP-HPLC. The linear and cyclic peptides were purified with a 10–50% B and 10–90% B gradient, respectively, over 15 min. The peptides eluted at 9.8 and 12.5 min, respectively, with a 12% overall yield for the pure CTP. Linear NH_2-pro-Pip-pro-Pro-COOH: ESI-TOF/MS: (*m/z*) Calcd for $C_{21}H_{32}N_4O_5H$ [M + H+], $C_{21}H_{32}N_4O_5Na$ [M + Na+]: 421.52 and 443.50, respectively. Obsd 421.35, 443.43, respectively.

Table II Cyclic Tetrapeptides – NMR Chemical Shifts

	NH	αH	βH	γH	δH	εH	Others	Conformation
c[pip-Pro-pip-Pro]								TTCT
D-pip[1]		5.38	1.49, 2.13	1.63, 2.33	1.50, 1.55	3.70, 3.79		
L-Pro[2]		5.11	1.66, 2.24	1.60, 1.84	3.41, 3.49			
D-pip[3]		4.81	1.12, 1.91	1.54, 2.61	1.37,1.77	3.51,3.77		
L-Pro[4]		5.52	2.08, 2.30	1.90	3.54, 3.71			
c[pro-Pro-pro-NMethAla]								TTTT
D-pro[1]		4.50	1.66, 2.41	1.86, 2.06	3.12, 3.43			
L-Pro[2]		4.74	2.00, 2.09	1.90, 2.22	3.41, 4.01			
D-pro[3]		4.60	1.86, 2.29	2.00, 2.09	3.56, 4.00			
N-methyl-l-Ala[4]		3.49	1.43				NCH_3 3.21	
c[Ala-Pro-pip-Pro]								TTCT
L-Ala[1]	7.73	4.86	1.52				NH $\Delta\delta/\Delta T$ (10^{-3} ppm/K) 2.2	
L-Pro[2]		4.67	1.89, 2.35	2.11, 1.90	3.58, 3.76			
D-pip[3]		5.10	1.44, 2.23	1.70, 1.64	1.32	3.07, 3.70		
L-Pro[4]		4.89	2.11, 2.33	1.80, 1.81	3.59, 3.82			
c[pro-Pip-pro-Pro]								T-T-
D-pro[1]		4.56	1.97, 2.18	1.83, 1.97	3.69, 3.82			
L-Pip[2]		4.54	1.82, 2.01	1.82	1.60, 1.69	3.36, 3.48		
D-pro[3]		4.52	1.95, 2.21	1.83, 2.08	3.72, 3.84			
L-Pro[4]		4.75	2.01, 2.27	2.01	3.46, 3.65			

Proton Chemical Shifts (ppm) of c[pip-Pro-pip-Pro], c[pro-Pro-pro-NMe-Ala], c[Ala-Pro-pip-Pro], c[pro-Pip-pro-Pro] in $CDCl_3$ (at 25°C except for c[pro-Pro-pro-NMe-Ala] which was measured at −20°C). For c[pro-Pip-pro-Pro] ppms are for the major conformation observed. NMR verified amide bond conformations listed (t, *trans*; c, *cis*, first letter refers to amide bond between first and second amino acid in first column).

c[pro-Pip-pro-Pro] was analyzed by ^{1}H, COSY, TOCSY, NOESY NMR (500 MHz, CDCl3, 25°C) Table II; ESI-TOF/MS: (m/z) calcd. for $(C_{21}H_{30}N_4O_4)H$ [(M + H)+)], $(C_{21}H_{30}N_4O_4)Na$ [(M + Na)+)], $2(C_{21}H_{30}N_4O_4)H$ [(D + H)+], $2(C_{21}H_{30}N_4O_4)Na$ [(D + Na)+]: 403.51, 425.49, 806.01, 827.99 respectively. Obsd 403.4, 425.5, 805.81, 827.3

c[pip-Pro-pip-Pro]. The linear peptide NH_2-pip-Pro-pip-Pro-COOH was synthesized by standard SPPS as described above by coupling Fmoc-D-pip, Fmoc-L-Pro, and Fmoc-D-pip consecutively to L-Pro-trityl-resin. After removal of the N-terminal Fmoc group, the linear tetrapeptide was released by treatment with 2% TFA in DCM from the resin support followed by purification on RP-HPLC. After a 3-day cyclization with HOBt, 3*M* equivalents of PyBOP and DIEA were added for one additional day. The linear and cyclic peptide were purified in a 10–90% B gradient over 15 min and eluted at 10.1 and 16.5 min, respectively, with a 25% overall yield for the pure CTP. Linear NH_2-pip-Pro-pip-Pro-COOH ESI-TOF/MS: (*m/z*) Calcd for $C_{22}H_{34}N_4O_5H$ [(M + H)+], $C_{22}H_{34}N_4O_5Na$ [(M + Na)+], $2(C_{22}H_{34}N_4O_5)H$ [(D + H)+], $2(C_{22}H_{34}N_4O_5Na$ [(D + Na)+]: 435.55, 457.54, 870.09, 891.09, respectively. Obsd 435.4, 457.4, 869.3, 891.4, respectively. c[pip-Pro-pip-Pro] was analyzed by ^{1}H, COSY, TOCSY, NOESY NMR (500 MHz, CDCl3, 25°C) Table II; ESI-TOF/MS: (*m/z*) Calcd for $C_{22}H_{32}N_4O_4H$ [(M + H)+], $2(C_{22}H_{32}N_4O_4H$ [(D + H)+], $2(C_{22}H_{32}N_4O_4Na$ [(D + Na)+]: 417.53, 834.03, 856.03 respectively; Obsd 417.5, 833.7, 855.9, respectively.

c[Ala-Pro-pip-Pro]. The linear peptide NH_2-Ala-Pro-pip-Pro-COOH was synthesized by standard SPPS as described earlier by coupling Fmoc-D-pip, Fmoc-L-Pro, and Fmoc-L-Ala consecutively to L-Pro-trityl-resin. After removal of the *N*-terminal Fmoc group, the linear tetrapeptide was released by treatment with 2% TFA in DCM from the resin support followed by purification on RP-HPLC. After a 3-day cyclization with HOBt, 3*M* equivalents of PyBOP and DIEA were added for one additional day. The linear and cyclic peptide were purified in a 10–90% B gradient over 15 min and eluted at 10.0 and 15.0 min, respectively, with an 18% overall yield for the pure CTP. Linear NH_2-Ala-Pro-pip-Pro-COOH ESI-TOF/MS: (*m/z*) calcd. for $C_{19}H_{30}N_4O_5H$ [(M + H)+], $C_{19}H_{30}N_4O_5Na$ [(M + Na)+], $2(C_{19}H_{30}N_4O_5H$ [(D + H)+], $2(C_{19}H_{30}N_4O_5Na$ [(D + Na)+]: 395.48, 417.47, 789.46, 811.45, respectively. Obsd 395.3, 417.3, 789.3, 811.3, respectively. c[Ala-Pro-pip-Pro] analyzed by ^{1}H, COSY, TOCSY, NOESY NMR (500 MHz, CDCL3, 25C) Table II; ESI-TOF/MS: (*m/z*) Calcd. for $C_{19}H_{28}N_4O_4H$ [(M + H)+], $2(C_{19}H_{28}N_4O_4)H$ [(D + H)+], $2(C_{19}H_{28}N_4O_4)Na$ [(D + Na)+]: 377.46, 753.93,775.36, respectively. Obsd 377.3, 753.5, 775.6, respectively.

NMR Structural Analysis

^{1}H, COSY, TOCSY, and NOESY NMR data were collected on c[pro-Pro-pro-NMe-Ala], c[pro-Pip-pro-Pro], c[pip-Pro-pip-Pro], and c[Ala-Pro-pip-Pro]. NMR spectra were recorded with a Varian Inova-600 (Varian, Palo Alto, CA) spectrometer and the data processed with VNMR software. The total correlation (TOCSY) spectra were recorded using an MELV-17 mixing sequence of 120 ms flanked by two 2 ms trim pulses. Phase-sensitive 2D spectra were obtained by employing the hypercomplex method. A total of 2 × 256 × 2048 data matrixes with 16 scans per t1 increment were col-

lected. Gaussian and sine-bell apodization functions were used in weighting the t2 and t1 dimensions, respectively. After two-dimensional Fourier transformation, the 2048 × 2048 frequency domain representation was phase and baseline corrected in both dimensions.

The NOESY spectrum resulted a 2 × 256 × 2049 data matrix with 32 scans per t1 increment. Spectra were recorded with 250 and 450 msec mixing time. The use of a 450 msec mixing time afforded a better result. The hypercomplex method was used to yield phase-sensitive spectra. The time-domain data were zero filled to yield a 2048 × 2048 data matrix and were processed in a similar way as the 2D TOCSY spectrum described above. Chemical shift data for the four cyclic peptides in $CDCL_3$ at −20°C is detailed in Table II. ROESY NMR spectra were obtained on all four peptides to see if more through-space cross peaks could be observed, possibly absent in NOESY spectra due to the effect of molecular mass on correlation time, but no new peaks were observed (data not shown).

A sodium-dimer model of c[pro-Pro-pro-NMe-Ala] was developed to explain an NOE peak between the *N*-methyl hydrogens and the proceeding Dpro-Cγ hydrogen. Two all-trans amide bond DFT structures were used to sandwich a Na atom between them. All NOE constraints were imposed with a 100 kj/mol-Å^2 penalty if more than 4 Å apart. This locked all amide bonds in the trans configuration and set a constraint between the *N*-methyl$_i$ to D-proγ_{i+1}. Spring constants of 100 kj/mol-Å^2 were also imposed between the sodium and Cα atoms if more than 5 Å apart. A conformational search was done using the OPLS-2001 force field in vacuum taking 1000 Monte-Carlo steps. The lowest energy structure satisfied all NOE peaks was found and is shown in Figure 2b.

Overlap of Structures With Reverse-Turn Classes From PDB

Recently Tran et al. elucidated nine sets of four vectors which represent almost all (∼90%) of the relative orientations of the four Cα-Cβ bonds found in reverse turns in the PDB.[37] The ability of our CTPs NMR conformation to mimic reverse turns was established by how well the NMR experimental structure had bonds overlapping the nine sets of four vectors established by Tran et al.[37] as representative of reverse-turn Cα-Cβ bonds. It was found that overlapping a Cα-Cβ vector of a Tran et al. cluster with a C—H bond on a CTP gave an undesired biased overlap compared to overlapping a C—C bond in the CTP. Even if the C—H bond was oriented in the correct direction, the difference in bond length from a C—H and C—C bond increased the total RMSD of the overlap. Therefore, each Tran cluster of four vectors was converted into its own subcluster by changing the bond lengths combinatorially to represent C—C and C—H bonds (1.52 Å and 1.10 Å, respectively) keeping the four Cα atoms in place. There were 16 sets of 4 vectors for each initial set, and a total of 144 sets of 4 vectors. This enabled us to directly overlap possible combinations of C—H and C—C bonds on our CTPs more accurately. These four vector structures were overlapped with the all trans NMR structure c[pro-Pro-pro-NMe-Ala] to find rigid structures that could serve as privileged scaffolds. The program FOUNDATION was used for overlapping using a clique-finding algorithm to exhaustively overlap bonds in order.[38] Searches were done which looked for 3- and 4-bond overlaps with RMSD of all 6, or 8 atoms, respectively of less than 0.3 Å, 0.5 Å, and 0.7 Å.

RESULTS AND DISCUSSION

Conformational Search of CTPs

To screen CTPs as reverse-turn mimics to act as probes for molecular recognition or as potential therapeutics, computational studies were used to find CTPs that had similar stable conformations in both vacuum and water. The objective was reverse-turn mimics whose unique conformers were retained in both the hydrophilic bulk water and while being bound in a hydrophobic environment, such as a receptor recognition site. Single and double amino acid substitutions of the parent peptide c[Pro-pro-Pro-pro][25] were simulated to determine how the noncoded amino acids NMe-Ala,[12] Pip, and Aib would affect the *cis/trans/cis/trans* conformation of amide bonds in CTPs. This resulted in 9 CTPs which were initially investigated by performing Monte-Carlo conformational searches (MCCS) in both vacuum and water (Table I). All 12 bonds in the cyclic peptide-chain macrocycle were rotated, including the four amide bonds. In addition the proline and Pip side chains were allowed to sample different side-chain ring puckers. Eight of the nine CTPs were found to have the same low-energy conformation in both vacuum and water by MCCS (Table I). c[Pro-pro-NMe-Ala-NMe-Ala] was the only CTP with different conformers in vacuo and in water, and was not studied further. As a control for adequate sampling, all compounds had their mirror-image counterparts conformationally searched in the same manner. An identical set of low-energy mirror-image conformers were found as expected suggesting adequate sampling. In addition, for all CTPs, MCCS runs found all 16 possible *cis/trans*-amide bond conformers. The expected puckering of the proline and pipecolic rings, up and down, or boat and chair, respectively, was also observed (data not shown). All these observations suggested that the conformational hyperspace available to these CTPs was adequately sampled.

CTPs have a strained macrocyclic ring that can cause their amide bonds to be significantly divergent from the ideal 180° or 0° ω-torsion values. Therefore, a quantum treatment of this system was more appropriate than molecular mechanical, which is inadequately parameterized for nonideal amide-bond torsions. For this reason, the lowest and second-lowest energy conformations for these eight structures from the MCMM calculations were minimized with DFT in both vacuum and H_2O.

In both the MCCS and DFT calculations, all the CTPs with Pip (c[Pro-pro-Pro-pip], c[pip-Pro-pip-Pro], c[Pro-pro-Pip-pip] adopted all *trans*-amide bond conformations (as did their enantiomers) (Table I). The $\Delta\Delta G$ between the lowest energy and second-lowest energy conformation for these three CTPs was significantly greater (5–9 kcal) in vacuo than in water because their all *trans*-amide conformation has a net dipole of ∼0, which is favored in vacuum, while the

second-lowest energy conformers with a higher dipole paid an energetic cost of solvation in vacuum compared to water. The peptide c[pro-Pro-pro-NMe-Ala] was also shown to adopt an all *trans*-amide conformation by both MCCS and DFT in both vacuum and water. CTPs that adopt this all *trans*-amide bond conformation in water could be expected to rigidify even further when bound in a nonpolar binding site in a receptor. All four of these CTPs low-energy all *trans* conformations was more than 5 kcal/mol more stable than their second-lowest energy conformation in both water and vacuum as determined by DFT (Table I). The fact that all four of these structures were found computationally to have all *trans*-amide bonds is not surprising given that most crystal structures of CTPs are in either the all *trans* or an alternating *cis*/*trans*/*cis*/*trans* conformation (Cambridge Structural Database 2007 analysis). None of the other CTPs were shown by DFT to have as stable a structure, and were not further experimentally explored.

The three rigid CTPs c[pro-Pro-pro-NMe-Ala], c[pro-Pip-pro-Pro], and c[pip-Pro-pip-Pro] all have tertiary amides for each amino acid and, therefore, have no NH's available for intramolecular hydrogen bonding. After NMR structural analysis, the peptide c[pip-Pro-pip-Pro] was found to have a *trans-trans-cis-trans* amide bond conformation and c[Ala-Pro-pip-Pro] was synthesized by SPPS as described earlier in an attempt to incorporate a hydrogen bond between the alanine NH and either the preceding or subsequent proline carbonyl to further stabilize this *trans-trans-cis-trans* structure.

Synthesis and NMR Characterization

The linear peptides NH_2-pro-Pip-pro-Pro-COOH, NH_2-pip-Pro-pip-Pro-COOH, NH_2-pro-NMe-Ala-pro-Pro-COOH, and NH_2-Ala-Pro-pip-Pro-COOH were synthesized by standard solid phase peptide synthesis (SPPS), purified by RP-HPLC, cyclized in a dilute 0.1 m*M* DMF solution to prevent dimerization, and again purified by RP-HPLC. The total yield for the cyclic peptides ranged between 11–22%. All four CTPs c[pro-Pro-pro-NMe-Ala], c[Pro-pip-Pro-pro], c[pip-Pro-pip-Pro], and c[Pro-pro-Pro-Ala] were characterized by ^{1}H, COSY, TOCSY, and NOESY NMR (Table II) and mass spectra. The NOESY data was used to determine the *cis/trans* conformation of the peptide bonds. In a Pro-pro or Pro-pro N-methylated dipeptide sequence, a NOE peak between succeeding CαH-CαH and CαH-CδH indicates a *cis*- and *trans*-amide bond, respectively. This holds true for Pro-pip and pro-Pip as well, except the *trans* NOE observed is between a Cα and the succeeding Cε.

Proton chemical shifts of c [Ala-Pro-pip-Pro] were assigned completely by analysis of TOCSY (Figure 1d) and COSY spectra. The Ala residue was identified first by the spin propagation from NH through β-CH3. The correlated proton resonances at 3.0–3.8 ppm were unambiguously assigned to δ and ε protons of the Pro and pip residues (Figure 1e). Sequential assignment of c[Ala^1-Pro^2-pip^3-Pro^4] was obtained by using the NH(i) -αH(i-1), δ,εH(i)-αH(i-1) fingerprint region of the NOESY spectrum (Figure 1c). Observed NH(Ala^1)-αH(Pro^4), εH(pip^3)-αH(Pro^2) and δH(Pro^2)-αH(Ala^1) NOE's indicated the *trans* conformation of the peptide bonds between these adjacent residues. However, a strong αH(Pro^4)-αH(pip^3) peak revealed a *cis*-amide bond conformation at the Pro4-pip^3 segment, hence a *trans-trans-cis-trans* conformation. NOESY spectrum of c[pip^1-Pro^2-pip^3-Pro^4] also suggested a *trans-trans-cis-trans* amide conformation as evident by the observed αH(Pro^2)-αH(pip^1), εH(pip^3)-αH(Pro^2), δH(Pro^4)-αH(pip^3) and εH(pip^1)-αH(Pro^4) NOE's in Figure 1b. Observed δ(i)-α(i-1) cross peaks in addition to the NCH$_3$(Ala^4)-αH(Pro^3) NOE peak in Figure 1a indicated an all *trans*-amide bond conformation appeared in c[pro^1-Pro^2-pro^3-NMethAla^4]. NOESY spectrum for c[pro^1-Pip^2-pro^3-Pro^4] revealed two conformations, the major conformation (80% in $CDCL_3$ at 25°C) only reveals two *trans*-amide bonds at pro^1-Pip^2 and pro^3-Pro^4. Neither a typical *trans*- nor *cis*-bond was seen between the Pip^2-pro^3 and Pro^1-Pro^4 (Supplementary Material). The minor conformation revealed trans bonds between pro^1-Pip^2, Pip^2-pro^3, and Pro^1-Pro^4 but neither a typical *trans*- nor *cis*-bond was seen between the Pip^2-pro^3.

Complete assignments for each residue of c[Ala^1-Pro^2-pip^3-Pro^4], c [pip^1-Pro^2-pip^3-Pro^4], c[pro^1-Pro^2-pro^3-NMethAla^4], and c[pro^1-Pip^2-pro^3-Pro^4] are shown in Table II. The temperature dependences of the Ala^1 amide proton shows evidence of intramolecular hydrogen bonds in c[Ala^1-Pro^2-pip^3-Pro^4]. The $\Delta\delta/\Delta T$ values of 2.2×10^{-3} ppm/K indicated that amide protons were somewhat shielded from solvent (Table II). Interestingly, it was found that the chemical shift differences for the two ε-pip^3 protons were quite large ($\Delta\delta = 0.63$ ppm). The intramolecular hydrogen bond may involve the carbonyl group of the pip^3-Pro^4 amide bond due to the *cis*-amide bond conformation. In such a case, one of the ε-pip^3 proton was fixed in the shielding zone of peptide bonds due to the difference in orientation of these two ε protons with respect to the carboxyl group of neighboring residues, which leads to a strong nonequivalence in chemical shift.

c[pro-Pro-pro-NMe-Ala] was the only compound with enough NOESY NMR data to validate a single low-energy rigid conformation supported by computational conformational searches (Tables I and II, Figure 1a) and was, therefore, the best prospect to screen as a reverse-turn priviliged scaffold. A conformational search of c[pro-Pro-pro-NMe-Ala] was performed with the 8 NMR constraints pro1$_\alpha$-Pro2γ_1,

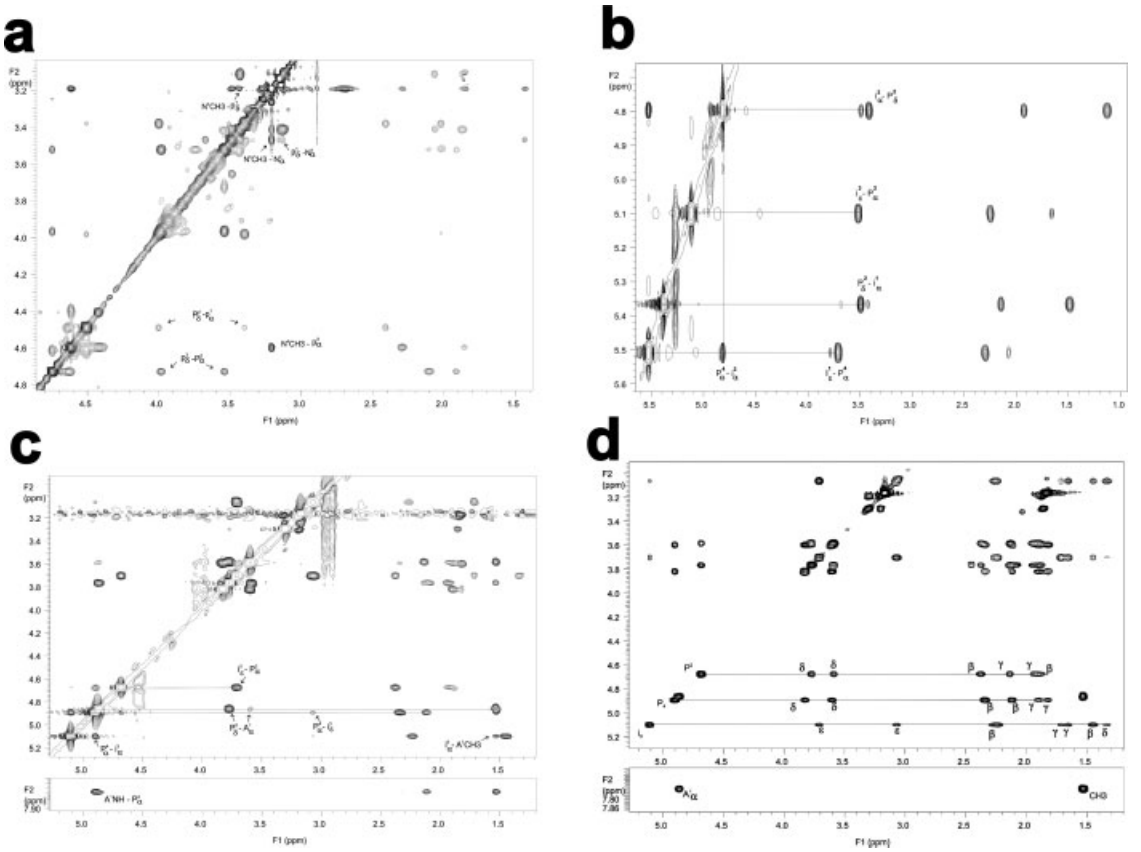

FIGURE 1 NOESY NMR data for the CTPs in $CDCl_3$. NMR data revealed an all *trans* conformation for c[pro^1-Pro^2-pro^3-NMe-Ala^4] (a), *trans-trans-cis-trans* for both c[pip^1-Pro^2-pip^3-Pro^4] (b) and c[Ala^1-Pro^2-pip^3-Pro^4] (c). Expansions of the 600-MHz 2D NOESY spectra of αH- aliphatic regions of c[pro^1-Pro^2-pro^3-NMe-Ala^4] at −20°C (a), αH- aliphatic regions of c[pip^1-Pro^2-pip^3-Pro^4] at 25°C (b), αH-aliphatic (c, top) and the NH(Ala^1) -αH $-CH_3$ region (c, bottom) of c[Ala^1-Pro^2-pip^3-Pro^4] at 25°C. TOCSY spectra was used to assign peaks as exemplified by the αH-aliphatic (d, top), and NH(Ala^1) -αH $-CH_3$ region (d, bottom) of the phase-sensitive 600-MHz 2D TOCSY spectra of c[Ala^1-Pro^2-pip^3-Pro^4] in $CDCl_3$ at 25°C. (A = L-Alanine, P = L-Proline, p = D-proline, *N* = *N*-methyl-L-Alanine, *I* = L-pipecolic acid, *i* = D-pipecolic acid).

pro1$_\alpha$-Pro2γ_2, Pro2α-pro3γ_1, Pro2α-pro3γ_2, pro3α-NMeAla4Nmethyl, NMeAla4α-pro1γ_1, and NMeAla4α-pro1γ_2 constrained within 4 Å of each other, and only the all *trans*-amide bond conformer was found. Both the initial MCMM search and DFT minimized structures of c[pro-Pro-pro-NMe-Ala] had an all *trans*-amide bond conformation with the NOE constrained atoms ∼2.2 Å apart. The all *trans* conformer has a dipole of ∼0 with the macrocycle adopting a boat conformation. The two proline rings opposite each other are both on the same side of the macrocycle and oriented perpendicularly to it, with their carbonyls likewise pointing perpendicularly to the same side of the macrocycle. The proline in between these two and the N—Me—alanine opposite are oriented similarly, but on the other face of the macrocycle (Figure 2a). All the prolines are puckered towards the center of the macrocycle.

A sodium ionic dimer model of c[pro-Pro-pro-NMe-Ala], as seen by Mass Spec, was developed to explain a NOE peak between the *N*-methyl and proceding D-pro Cγ hydrogens. A conformational search restricting a Na+ atom between two cyclic monomers with NOE constraints resulted in a low-energy structure that confirmed the *N*-methyl$_i$ to D-proγ_{i+1} NOE (Figure 2b). The model also predicted a NOE between the pro3δ-Pro2γ which we then also confirmed in the NOE spectra. We then proceeded to screen the all-trans c[pro-Pro-pro-NMe-Ala] monomer as a reverse-turn mimic.

Reverse-Turn Mimetic Screen

Historically, reverse turns have been classified by the 4 torsions of the i+1 and i+2 residues, i.e., the φ and ψ of the second and third residues of the reverse turn. However, there

are two torsions, ψ of the first residue and φ of the fourth residue that effect orientation of the first and fourth side chains that were not taken into account in this traditional reverse-turn nomenclature. It has been shown that reverse turns in the same classical-turn type can differ in the orientation of their side chains.[37] Because reverse turns are usually recognized in biological systems by their relative side-chain orientation and not direct interactions with their backbones, the classical classification method is not optimal. Recently, Tran et al.[37] have elucidated nine classes of orientations of the four consecutive Cα-Cβ bonds of a reverse turn that represent the vast majority ($\sim$90%) of reverse turns found in the PDB. These nine classes were used to screen our semi-rigid CTPs as reverse-turn mimics.

The DFT-minimized all *trans* conformer for c[pro-Pro-pro-NMe-Ala] was tested for overlap with the nine reverse-turn clusters of Tran et al.[37] (Table III). An excellent overlap was found for all four Cα-Cβ bonds of cluster 6 of Tran et al.'s with a deviation of 0.57 Å RMSD (Figure 2a). Cluster 6 is largely made up of classical Type I β-turns.[37] The Cα-Cβ bonds of the N-Me-Ala, the succeeding D-pro, and the succeeding Pro overlap the i, i+1, and i+2 Cα-Cβ bonds of cluster 6, while one of the Cγ-H bonds on the first residue, Pro, overlaps that last Cα-Cβ i+3 bond. If used as a mimic, the side-chain substituents mimicked by the 3 Cα-Cβ bonds of c[pro-Pro-pro-NMe-Ala] would also have at least one of their later side-chain torsion angles locked in place. Therefore, this CTP would likely not work to mimic a glycine or alanine at one of these positions due to the extra steric bulk of the proline exocyclic ring. However, if a larger side chain branched off the c[pro-Pro-pro-NMe-Ala] structure at one of the two Cβ-H bond, this would be equivalent to locking not only the Cα-Cβ bond, but also the Cβ-Cγ of the side chain. If the correct side-chain conformation followed the ring up to Cβ-Cγ, and then branched off one of the two Cγ-H bonds of the proline ring, this would in essence rigidify the "side chains" Cα, Cβ, Cγ, and Cδ atoms. As mentioned earlier, this could probe the receptor with a very well-determined side-chain conformation to assist in elucidating an unknown bound conformation of the bioactive parent peptide.

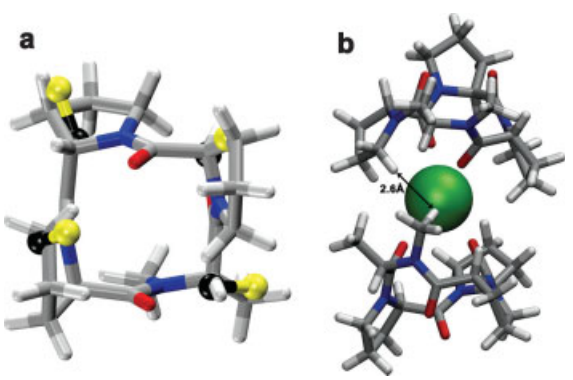

FIGURE 2 Overlap of CTP with Cα-Cβ bonds of Cluster 6. The all *trans* c[pro-Pro-pro-NMe-Ala] is overlapped (0.57 Å RMSD) by all 4 Cα-Cβ bonds in Tran et al.'s cluster 6 which mainly represents classical β-turn Type I. The Cα and Cβ atoms are in black and yellow respectively (a). A dimer model of 2c[pro-Pro-pro-NMe-Ala]●Na that has the *N*-methyl hydrogen within 3 Å of the proceeding proγ hydrogen of the other monomer justifying an observed NOE peak (b).

Table III c[pro-Pro-pro-*N*-Methyl-L-Ala] Reverse-Turn Overlaps

c[pro-Pro-pro-*N*-Methyl-L-Ala] Mimics of Reverse Turns			
Tran Cluster no. Overlapped	Analogous Classical B-turn(s)	No. of Cα-Cβ Bonds Overlapped	RMSD to Tran Cluster (Å)
6	I	4	0.57
2	II	3	0.22
3	I and IV	3	0.21
4	II and IV	3	0.28
6	I	3	0.26
7	II and IV	3	0.26
8	VIII	3	0.24

Results of overlapping c[pro^1-Pro^2-pro^3-*N*-Methyl-L-Ala^4] all *trans* DFT structure with the 9 Tran reverse-turn Cα-Cβ vectors.

A short 1 ps dynamics run was done on c[pro-Pro-pro-NMe-Ala] using the Amber force field to estimate vibrational flexibility of the CTP at room temperature. The limited set of 200 conformers sampled effectively adopt the same ring conformation (Figure 3a). Trans β-turn clusters 2, 3, 4, 6, 7, and 8 (which are represented largely by classical β-turns types II, I and IV, II and IV, I, II and IV, and VIII, respectively) all had 3 bonds overlapped by a snapshot of the c[pro-Pro-pro-NMe-Ala] dynamics run with a RMSD of $<$0.3 Å (Figure 3b–g, Table III). This exemplifies the point of how well suited CTPs are at mimicking reverse turns. They inherently present a 180° reverse turn of consecutive four residues no matter which residues you pick as the first residue. In essence, therefore, every CTP has 4 "chances" of rotating and interacting with a receptor as a new reverse-turn mimic.

CONCLUSIONS

Having a diverse set of CTPs incorporating D and L proline that mimic reverse turns enables both useful probes for determining the optimal side-chain geometry and for reverse-turn recognition. c[Pro-pro-NMe-Ala-pro] was shown to adopt an all *trans* amide-bond conformation that could mimic all the Cα-Cβ bonds in the classical type I

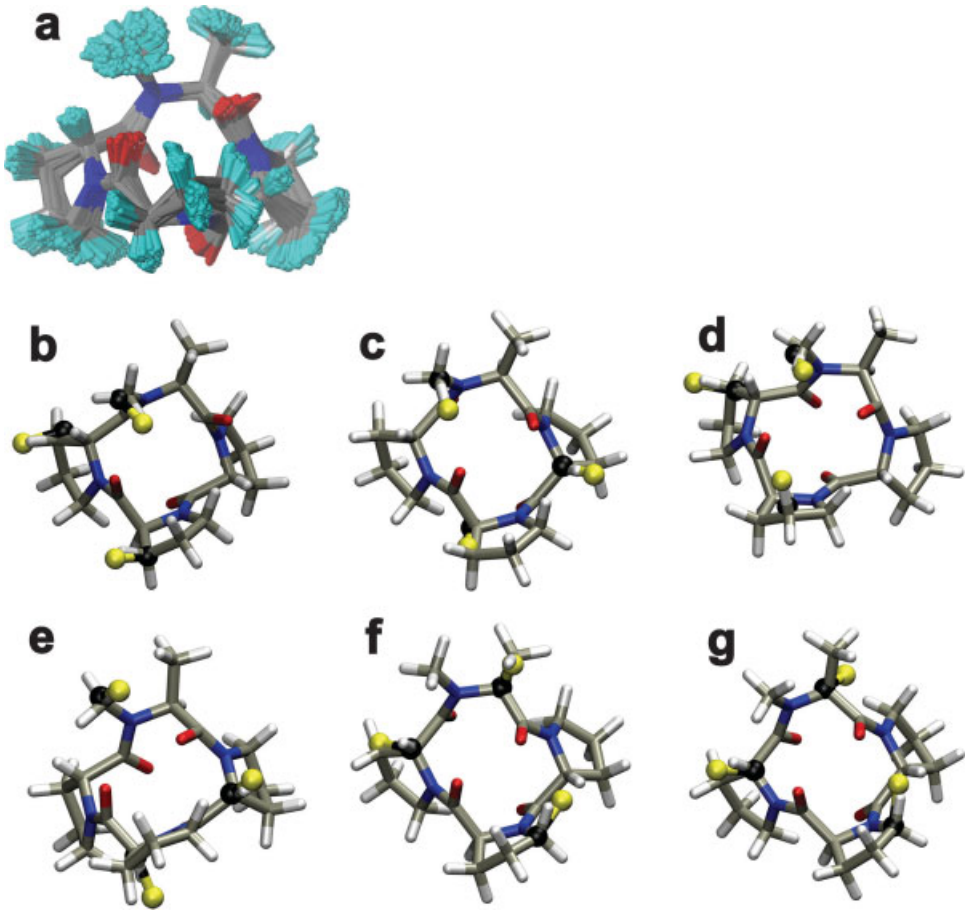

FIGURE 3 Overlap of Tran et al.'s cluster with snapshots from MD run. 200 Snapshots of the all *trans* c[pro-Pro-pro NMe-Ala] 1ps dynamics run (a) are overlapped (<0.3 Å RMSD) by 3 Cα-Cβ bonds in Tran et al.'s clusters 2, 3, 4, 6, 7, and 8 (b–g), respectively (which are represented largely by classical β-turns types II, I and IV, II and IV, I, II and IV, and VIII, respectively). The Cα and Cβ atoms are in black and yellow, respectively.

β-turns (Figure 2a), with the ability to lock out Cβ-Cγ and possibly even Cγ-Cδ torsions of three of the four side chains. In addition, c[Pro-pip-NMe-Ala-pro] could mimic 3 out of 4 of the Cα-Cβ bonds of Type I, II, IV, and VIII extremely well (Figure 3, Table III). CTPs can inherently mimic reverse turns well as exemplified by how many different turn types for which c[pro-Pro-pro-NMe-Ala] could mimic 3 of the 4 side chains. However, to mimic all four Cα-Cβ side chains of all the reverse turns, a library of many CTPs with varying *cis*/*trans*-amide bond torsions will be needed. Future work will include determination of the impact of methyl group for proton substitution on the CTP to disrupt or stabilize the conformations determined to be most stable by these studies.

Weijun Zhang provided useful help in peptide synthesis and Chris Ho useful guidance in the use of the FOUNDATION program. SBC acknowledges fellowship support from the Division of Biology and Biological Sciences, Washington University in St. Louis, Kauffman Cancer Research Pathway, and Washington University Center for Computational Biology Pathway.

REFERENCES

1. Richardson, J. S. Adv Protein Chem 1981, 34, 167–339.
2. Fairlie, D. P.; West, M. L.; Wong, A. K. Curr Med Chem 1998, 5, 29–62.
3. Halab, L.; Gosselin, F.; Lubell, W. D. Biopolymers 2000, 55, 101–122.
4. Kuntz, I. D. J Am Chem Soc 1972, 94, 4009–4012.
5. Rose, G. D.; Gierasch, L. M.; Smith, J. A. Adv Protein Chem 1985, 37, 1–109.
6. Bunin, B.; Plunkett, M.; Ellman, J. Proc Natl Acad Sci USA 1994, 91, 4708–4712.
7. Ripka, W. C.; DeLucca, G. V.; Bach, A. C., II; Pottorf, R. S.; Blaney, J. M. Tetrahedron 1993, 49, 3593–3608.
8. Ripka, W. C.; Lucca, G. V. D.; Bach, A. C., II; Pottorf, R. S.; Blaney, J. M. Tetrahedron 1993, 49, 3609–3628.
9. Horton, D. A.; Bourne, G. T.; Smythe, M. L. Chem Rev 2003, 103, 893–930.

10. Breinbauer, R.; Vetter, I. R.; Waldmann, H. Angew Chem Int Ed Engl 2002, 41, 2879–90.
11. Muller, G. Drug Discov Today 2003, 8, 681–691.
12. Chalmers, D. K.; Marshall, G. R. J Am Chem Soc 1995, 117, 5927–5937.
13. Takeuchi, Y.; Marshall, G. R. J Am Chem Soc 1998, 120, 5363–5372.
14. Spath, J.; Stuart, F.; Jiang, L.; Robinson, J. A. Helv Chim Acta 1998, 81, 1726–1738.
15. Muller, G.; Gurrath, M.; Kurz, M.; Kessler, H. Proteins 1993, 15, 235–251.
16. Reaka, A. J. H.; Ho, C. M. W.; Marshall, G. R. J Comput-Aided Mol Des 2002, 16, 585–600.
17. Adessi, C.; Soto, C. Curr Med Chem 2002, 9, 963–978.
18. Gallo, S. A.; Wang, W.; Rawat, S. S.; Jung, G.; Waring, A. J.; Cole, A. M.; Lu, H.; Yan, X.; Daly, N. L.; Craik, D. J.; Jiang, S.; Lehrer, R. I.; Blumenthal, R. J Biol Chem 2006, 281, 18787–18792.
19. Darkin-Rattray, S. J.; Gurnett, A. M.; Myers, R. W.; Dulski, P. M.; Crumley, T. M.; Allocco, J. J.; Cannova, C.; Meinke, P. T.; Colletti, S. L.; Bednarek, M. A.; Singh, S. B.; Goetz, M. A.; Dombrowski, A. W.; Polishook, J. D.; Schmatz, D. M. Proc Natl Acad Sci USA 1996, 93, 13143–13147.
20. Walton, J. D. Proc Natl Acad Sci USA 1987, 84, 8444–8447.
21. Yoshida, H.; Sugita, K. Jpn J Cancer Res 1992, 83, 324–328.
22. Itazaki, H.; Nagashima, K.; Sugita, K.; Yoshida, H.; Kawamura, Y.; Yasuda, Y.; Matsumoto, K.; Ishii, K.; Uotani, N.; Nakai, H.; et al. J Antibiot (Tokyo) 1990, 43, 1524–1532.
23. Che, Y.; Marshall, G. R. J Med Chem 2006, 49, 111–124.
24. Mastle, W.; Weber, T.; Thewalt, U.; Rothe, M. Biopolymers 1989, 28, 161–174.
25. Ovchinnikov, Y. A.; Ivanov, V. T. In The Proteins; Neurath, H.; Hill, R. L., Eds; Academic Press: New York, 1982; Vol. 5, pp 307–642.
26. Loiseau, N.; Gomis, J. M.; Santolini, J.; Delaforge, M.; Andre, F. Biopolymers 2003, 69, 363–385.
27. Kessler, H.; Hessler, R. G. G.; Gurrath, M.; Muller, G. Pure Appl Chem 1996, 68, 1201–1205.
28. Chang, G.; Guida, W. C.; Still, W. C. J Am Chem Soc 1989, 111, 4379.
29. Saunders, M.; Houk, K. N.; Wu, Y.-D.; Still, W. C.; Lipton, M.; Chang, G.; Guida, W. C. J Am Chem Soc 1990, 112, 1419–1427.
30. Still, W. C.; Tempczyk, A.; Hawley, R. C.; Hendrickson, T. J Am Chem Soc 1990, 112, 6127–6129.
31. Macromodel, 7.2; Schrodinger, Inc.: Portland, Oregon, 2001.
32. Jorgensen, W. L.; Maxwell, D. S.; Tirado-Rives, J. J Am Chem Soc 1996, 118, 11225–11236.
33. Kaminski, G. A.; Friesner, R. A.; Tirado-Rives, J.; Jorgensen, W. L. J Phys Chem B 2001, 105, 6474–6487.
34. Wong, M. W.; Wiberg, K. B.; Frisch, M. J. J Chem Phys 1991, 95, 8991.
35. Wong, M. W.; Wiberg, K. B.; Frisch, M. J. J Am Chem Soc 1992, 114, 6.
36. Novabiochem, Catalog: Synthesis Notes. 2006/2007; p 3.4.
37. Tran, T. T.; McKie, J.; Meutermans, W. D.; Bourne, G. T.; Andrews, P. R.; Smythe, M. L. J Comput Aided Mol Des 2005, 19, 551–566.
38. Ho, C. M. W.; Marshall, G. R. J Comput-Aided Mol Design 1993, 7, 3–22.